Increased Apical Targeting of Renal Epithelial Sodium Channel Subunits and Decreased Expression of Type 2 11β-Hydroxysteroid Dehydrogenase in Rats with CCl_4-Induced Decompensated Liver Cirrhosis

Soo Wan Kim,*† Uffe K. Schou,* Christian D. Peters,* Sophie de Seigneux,* Tae-Hwan Kwon,*‡ Mark A. Knepper,§ Thomas E.N. Jonassen,‖ Jørgen Frøkiær,* and Søren Nielsen*

**The Water and Salt Research Center, University of Aarhus, Aarhus, Denmark; †Department of Internal Medicine, Chonnam National University Medical School, Gwangju, Korea; ‡Department of Biochemistry and Cell Biology, School of Medicine, Kyungpook National University, Taegu, Korea; §Laboratory of Kidney and Electrolyte Metabolism, National Heart, Lung, and Blood Institute, National Institutes of Health, Bethesda, Maryland; and ‖Department of Pharmacology, The Panum Institute, University of Copenhagen, Copenhagen, Denmark*

It was hypothesized that dysregulation of renal epithelial sodium channel (ENaC) subunits and/or 11β-hydroxysteroid dehydrogenase (11βHSD2) may play a role in the increased sodium retention in liver cirrhosis (LC). Experimental LC was induced in rats by CCl_4 (1 ml/kg, intraperitoneally, twice a week) for 12 wk (protocol 1) or for 11 wk (protocol 2). In both protocols, one group of rats with cirrhosis showed significantly decreased urinary sodium excretion and urinary Na/K ratio (group A), whereas a second group exhibited normal urinary sodium excretion (group B) compared with controls, even though extensive ascites was seen in both groups of rats with cirrhosis. In group A, protein abundance of α-ENaC was unchanged, whereas β-ENaC abundance was decreased in the cortex/outer stripe of outer medulla compared with controls. The γ-ENaC underwent a complex change associated with increased abundance of the 70-kD band with a concomitant decrease in the main 85-kD band, corresponding to an aldosterone effect. In contrast, no changes in the abundance of ENaC subunit were observed in group B. Immunoperoxidase microscopy revealed an increased apical targeting of α-, β-, and γ-ENaC subunits in distal convoluted tubule (DCT2), connecting tubule (CNT), and cortical and medullary collecting duct segments in group A but not in group B. Immunolabeling intensity of 11βHSD2 in the DCT2, CNT, and cortical collecting duct was significantly reduced in group A but not in group B, and this was confirmed by immunoblotting. In conclusion, increased apical targeting of ENaC subunits combined with diminished abundance of 11βHSD2 in the DCT2, CNT, and cortical collecting duct is likely to play a role in the sodium retaining stage of liver cirrhosis.

J Am Soc Nephrol 16: 3196–3210, 2005. doi: 10.1681/ASN.2004080721

Renal sodium and water retention has been shown to be responsible for the development of ascites not only in patients with liver cirrhosis but also in experimental rats with cirrhosis. Atrial natriuretic peptide resistance (1), arginine vasopressin (AVP) (2), renin-angiotensin-aldosterone (3), and sympathetic nerve overactivity (4) have been shown to modulate renal tubular functions and have been considered to be involved mainly in sodium and water retention in liver cirrhosis. In kidneys of rats with cirrhosis, increased reabsorption of sodium and water in the distal nephron and collecting duct has been suggested to be one of the most important renal tubular dysfunctions involved in the pathogenesis of ascites (5–7). However, the underlying molecular and cellular mechanisms for the sodium retention are still incompletely understood.

In particular, the role of aldosterone in sodium retention and ascites formation in liver cirrhosis is still unclear. Previous studies demonstrated that plasma aldosterone levels were usually elevated in liver cirrhosis with ascites (8–10) and that spironolactone, a mineralocorticoid receptor antagonist, increased sodium excretion in these patients (11). This suggests that hyperaldosteronism is of major importance in the pathogenesis of sodium retention. The epithelial sodium channel (ENaC) is the major sodium transport pathway in the collecting duct (12), and both protein abundance and apical plasma membrane targeting of the ENaC subunits are regulated by hormonal stimulation, *e.g.*, aldosterone (13) and vasopressin (14). We therefore speculated that altered protein abundance and/or apical membrane targeting of ENaC subunits (α, β, and γ) may account for the increased sodium reabsorption in the collecting

Received August 31, 2004. Accepted August 9, 2005.

Published online ahead of print. Publication date available at www.jasn.org.

Address correspondence to: Dr. Søren Nielsen, The Water and Salt Research Center, Building 233/234, University of Aarhus, Aarhus, Denmark DK-8000. Phone: +45-8942-3046; Fax: +45-8619-8664; E-mail: sn@ana.au.dk

ISSN: 1046-6673/1611-3196

duct and sodium retention in liver cirrhosis. However, other investigators have demonstrated that plasma aldosterone levels were normal in patients who had cirrhosis and presented ascites and that sodium retention persisted despite the maintenance of plasma aldosterone levels within normal limits (9,15). Thus, it would also be possible that the increased sodium reabsorption in the distal nephron and collecting duct could be mediated by other regulatory mechanisms. The intracellular access of glucocorticoids to mineralocorticoid receptors (MR) is modulated by the type 2 isoform of 11β-hydroxysteroid dehydrogenase (11βHSD2). 11βHSD2 confers mineralocorticoid specificity in aldosterone-sensitive epithelia in the kidney by metabolizing glucocorticoids, thus protecting MR from inappropriate activation by glucocorticoid (16,17). Such protection is critical because the glucocorticoid cortisol circulates in a 100-fold molar excess to aldosterone *in vivo* and binds to MR with an affinity similar to aldosterone (18,19). The importance of the enzyme is illustrated by the clinical consequences of mutations (20,21) in the 11βHSD2 gene and by the use of inhibitors (22) of 11βHSD2, both of which lead to the syndrome of apparent mineralocorticoid excess, a rare form of hypertension with low plasma aldosterone and sodium retention. Thus, we speculated that an increased access of cortisol to the MR in a condition that demonstrated decreased activity/expression of 11βHSD2 could account, at least in part, for the enhanced aldosterone effect in decompensated cirrhosis, although plasma aldosterone levels are not increased.

The purposes of this study, therefore, were (*1*) to examine whether there are changes in the protein abundance and/or apical targeting of ENaC subunits in kidneys of rats with CCl_4-induced liver cirrhosis, (*2*) to examine whether there are changes in the protein abundance of 11βHSD2, (*3*) to examine whether there are changes in the protein abundance of other renal sodium transporters along the renal tubules (type 3 Na/H exchanger [NHE3] and Na-K-2Cl co-transporter [NKCC2]), and (*4*) to examine whether these changes are associated with changes in the urinary sodium excretion.

Materials and Methods

Experimental Protocols

Protocol 1 (12 Wk of CCl_4 Injection). Experiments were performed using male Munich-Wistar rats (200 to 250 g; Møllegard Breeding Centre, Ll. Skensved, Denmark). The animal protocols were approved by the boards of the Institute of Anatomy and Institute of Clinical Medicine, University of Aarhus, according to the licenses for use of experimental animals issued by the Danish Ministry of Justice. Liver cirrhosis ($n = 10$) was induced by intraperitoneal injections of a solution of CCl_4 in groundnut oil (1:1), 1 ml/kg body wt twice a week throughout the experimental period. Control rats ($n = 7$) received intraperitoneal injections of groundnut oil 0.5 ml/kg body wt. For accelerating the generation of cirrhosis, all rats (both control and CCl_4-treated groups) received phenobarbital in the drinking water (350 mg/L) throughout the whole experimental period (23). They were maintained in individual cages on a standard rodent diet (Altromin #1324; Altromin, Lage, Germany) and allowed free access to drinking water at all times. CCl_4-treated and control rats were pair fed. In the control group, rats were offered the amount of food corresponding to the mean intake of food that the CCl_4-treated rats consumed during the previous day.

During the last 3 d, the rats were subsequently maintained in the metabolic cages to allow urine collections for the measurements of Na^+, K^+, creatinine, and osmolality. The rats were killed for immunoblotting and immunohistochemical studies 12 wk after CCl_4 treatment. Rats were anesthetized with halothane (Halocarbon Laboratories, River Edge, NJ), and a large laparotomy was made. Peritoneal fluid volume was quantified in each rat by absorbing the ascites fluid into preweighed dry papers and reweighing the papers. The difference in weight represented the weight of the collected peritoneal fluid. Blood was collected from the inferior vena cava and analyzed for bilirubin, alanine aminotransaminase (ALT), Na^+, K^+, creatinine, osmolality, and plasma aldosterone concentration using methods described previously in detail (24). The right kidney was rapidly removed, dissected into three zones (cortex and outer stripe of outer medulla [OSOM], inner stripe of outer medulla [ISOM], and inner medulla) and processed for immunoblotting as described below. The left kidney was fixed by retrograde perfusion as described below.

Protocol 2 (11 Wk of CCl_4 Injection). To confirm the changes of subcellular redistribution of ENaC subunits in the sodium-retaining stage of liver cirrhosis observed in protocol 1, another set of CCl_4-treated rats ($n = 11$) and control rats ($n = 7$) was made. This protocol was identical to protocol 1, except that control and CCl_4-treated rats were monitored for 11 wk.

Subgroups in CCl_4-Treated Rats

CCl_4-treated rats displayed various renal responses in the renal sodium retention/excretion. Some rats showed markedly decreased urinary sodium excretion (sodium retaining stage, group A), whereas the others did not exhibit differences in urinary sodium excretion (maintenance stage, group B) compared with controls, even though all CCl_4-treated rats in both groups had a significant amount of ascites. Thus, we subdivided rats with liver cirrhosis into two groups (group A and group B), according to the urinary sodium excretion measured at the last day of the experiment (Figure 1).

Semiquantitative Immunoblotting

The dissected renal cortex/OSOM, ISOM, and inner medulla were homogenized (Ultra-Turrax T8 homogenizer; IKA Labortechnik, Staufen, Germany) in ice-cold isolation solution that contained 0.3 M sucrose, 25 mM imidazole, 1 mM EDTA, 8.5 μM leupeptin, and 1 mM PMSF (pH 7.2). The homogenates were centrifuged at $4000 \times g$ for 15 min at 4°C to remove whole cells, nuclei and mitochondria, and the supernatant was pipetted off and kept on ice. The total protein concentration was measured (Pierce BCA protein assay reagent kit; Pierce, Rockford, IL). All samples were solubilized at 65°C for 15 min in SDS-containing sample buffer. For confirming equal loading of protein, an initial gel was stained with Coomassie Blue. SDS-PAGE was performed on 9 or 12% polyacrylamide gels. The proteins were transferred by gel electrophoresis (BioRad Mini Protean II) onto nitrocellulose membranes (Hybond ECL RPN3032D; Amersham Pharmacia Biotech, Little Chalfont, UK). The blots were subsequently blocked with 5% milk in PBS-T (80 mM Na_2HPO_4, 20 mM NaH_2PO_4, 100 mM NaCl, and 0.1% Tween 20 [pH 7.5]) for 1 h and incubated overnight at 4°C with primary antibodies followed by incubation with anti-rabbit (P448; DAKO, Glostrup, Denmark), anti-mouse (P447; DAKO), or anti-sheep (1713–035-147; Jackson Laboratories, Bar Harbor, ME) horseradish peroxidase–conjugated secondary antibodies. The labeling was visualized by an enhanced chemiluminescence system (ECL or ECL+plus) and exposure

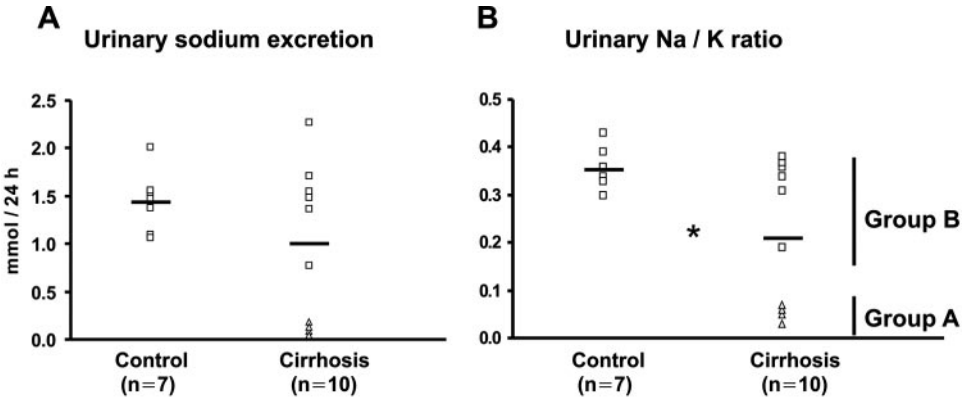

Figure 1. Urinary sodium excretion (A) and urinary Na/K ratio (B) from control and CCl_4-treated rats with cirrhotic (Cirrhosis) in protocol 1. (A) Urinary sodium excretion was similar in control and rats with CCl_4-induced cirrhosis. Four (△; group A) of the rats with CCl_4-induced cirrhosis showed markedly decreased urinary sodium excretion, whereas the other six rats (□; group B) remained similar compared with controls. (B) The urinary Na/K ratio was decreased in rats with cirrhosis, indicating increased aldosterone effectiveness in the distal nephron. *$P < 0.05$ *versus* control.

to photographic film (Hyperfilm ECL, Amersham). ECL films were scanned using an AGFA scanner (ARCUS II).

Immunohistochemistry

For perfusion fixation, a perfusion needle was inserted in the abdominal aorta of rats and the vena cava was cut to establish an outlet. Blood was flushed from the kidneys with cold PBS (pH 7.4) for 15 s before switching to cold 3% paraformaldehyde in 0.1 M cacodylate buffer (pH 7.4) for 3 min. The kidney and liver were removed and sectioned into 2- to 3-mm transverse sections and immersion fixed for an additional 1 h, followed by 3 × 10-min washes with 0.1 M cacodylate buffer of pH 7.4. The tissue was dehydrated in graded ethanol and left overnight in xylene. After embedding in paraffin, 2-μm sections of the tissue were cut on a rotary microtome (Leica Microsystems A/S, Herlev, Denmark).

Immunolabeling was performed on sections from paraffin-embedded preparation (2 μm thickness) using methods described previously in detail (24). For the liver histology, sections were stained with hematoxylin-eosin. Light microscopy was carried out with Leica DMRE (Leica Microsystems A/S).

Primary Antibodies

We used previously characterized polyclonal antibodies. Affinity-purified polyclonal antibodies against the renal sodium transporters/channels (24) (NHE3, NKCC2, thiazide-sensitive Na-Cl co-transporter [NCC], the ENaC subunits), aquaporin 2 (AQP2) and phosphorylated-AQP2 (p-AQP2) (25) were used. A sheep polyclonal antibody to 11βHSD2 (Chemicon, Temecula, CA) was commercially obtained. A mouse mAb against the Na,K-ATPase α1-subunit was provided by Dr. D.M. Fambrough (Johns Hopkins University Medical School, Baltimore, MD).

Statistical Analyses

Values are presented as means ± SE. Comparisons between two groups were made by the unpaired *t* test. Multiple comparisons among the groups were made by one-way ANOVA and *post hoc* Tukey HSD test. Multiple-comparisons tests were applied only when a significant difference was determined in the ANOVA ($P < 0.05$). $P < 0.05$ were considered significant.

Results

Changes of Urinary Sodium Excretion in CCl_4-Treated Rats (12-Wk Experiment, Protocol 1)

Table 1 shows the changes in liver and renal function in the 12-wk experiment (protocol 1). All of the CCl_4-treated rats had

Table 1. Changes in liver and renal function (12-wk experiment, protocol 1)[a]

	Control ($n = 7$)	Cirrhosis ($n = 10$)
Body weight (g)	312.0 ± 2.5	306.6 ± 11.6
Ascites (ml)	Nondetectable	17.3 ± 2.27
UO (μl/min)	8.5 ± 0.8	6.7 ± 0.5
P_{ALT}, U/L	51.4 ± 4.4	141.3±17.0[b]
$P_{bilirubin}$ (μmol/L)	2.1 ± 0.1	14.7 ± 2.1[b]
Pcr (μmol/L)	32.1 ± 2.0	25.3 ± 0.6[c]
Ccr (ml/min)	1.48 ± 0.09	1.29 ± 0.15
P_{Na} (mEq/L)	137.4 ± 0.8	135.5 ± 0.7
P_K (mEq/L)	5.7 ± 0.3	5.9 ± 0.2
U_{Na}×UO (mmol)	1.45 ± 0.12	0.96 ± 0.26
Na balance (mmol/d)	0.26 ± 0.12	0.92 ± 0.19[c]
FE_{Na} (%)	0.50 ± 0.03	0.33 ± 0.06[c]
FE_K (%)	33.7 ± 2.1	33.9 ± 2.4
Urine Na/K	0.36 ± 0.02	0.22 ± 0.05[c]

[a]Values are expressed as mean ± SE. These values are measured at the last day of experiments (12 wk). UO, urine output; P_{ALAT}, plasma alanine aminotransferase; $P_{bilirubin}$, plasma bilirubin; P_{Na}, plasma sodium; P_K, plasma potassium; Pcr, plasma creatinine; Ccr, creatinine clearance; U_{Na}×UO, rate of urinary sodium excretion; Na balance, the difference between dietary sodium intake and urinary sodium excretion in the 24 h; FE_{Na}, fractional excretion of sodium into urine; FE_K, fractional excretion of potassium into urine; Urine Na/K, urine sodium/potassium ratio.

[b]$P < 0.01$ *versus* control.

[c]$P < 0.05$ *versus* control.

large amount of ascites. Light microscopy of liver histology revealed well-established liver cirrhosis in all CCl_4-treated rats, in which the combination of nodular regeneration of liver cell plates surrounded by thick connective tissue septa with proliferating bile ducts define a picture of micronodular cirrhosis (data not shown) (26). Consistent with this, plasma concentrations of ALT and bilirubin were significantly increased in CCl_4-treated rats. Plasma creatinine levels were decreased, whereas renal creatinine clearance was not changed in CCl_4-treated rats. The 24-h urinary sodium excretion showed a decreased tendency in rats with cirrhosis. However, it was not statistically significant because the rats with cirrhosis showed wide variations in urinary sodium excretion (Figure 1A). Importantly, fractional excretion of sodium was decreased, and sodium balance was positive in CCl_4-treated rats. Urinary Na/K ratio was also decreased in CCl_4-treated rats. Moreover, the urinary osmolality (1934.0 ± 128 *versus* 1549.7 ± 71 mOsm/kgH_2O in controls; $P < 0.05$) and urine/plasma osmolality ratio were increased (6.6 ± 0.4 *versus* 5.1 ± 0.2 in controls; $P < 0.01$), indicating increased urinary concentration in CCl_4-treated rats.

Altered Protein Expression of ENaC Subunits in CCl_4-Treated Rats (12-Wk Experiment, Protocol 1)

In protocol 1, the protein abundance of α-ENaC was unchanged in cortex/OSOM, ISOM, and inner medulla in CCl_4-treated rats compared with controls (Figure 2). The abundance of β-ENaC was decreased in the cortex/OSOM, ISOM, and inner medulla (Figure 2). The γ-ENaC underwent a complex change associated with the appearance of a 70-kD band with a concomitant decrease in the main 85-kD band. These changes were prominent, especially in the CCl_4-treated rats associated with markedly decreased urinary sodium excretion (group A; Figure 2, arrows). The summary of analyses of normalized band densities is shown in Table 2.

In protocol 1 of 12 wk of CCl_4 treatment, four rats (group A) out of all of the CCl_4-treated rats showed markedly decreased urinary sodium excretion and urinary Na/K ratio, whereas the other six rats (group B) exhibited unchanged urinary sodium excretion and urinary Na/K ratio compared with controls (Figure 1, Table 3). Plasma aldosterone levels were markedly increased in group A, whereas the levels were decreased in group B compared with controls (Table 3). Thus, we subdivided CCl_4-treated rats into group A and group B according to urinary sodium excretion. To investigate whether the changes of protein abundance of ENaC subunits are related with the sodium retention, we performed additional immunoblot analysis in the cortex/OSOM (Figure 3). In group A, protein abundance of α-ENaC was unchanged, whereas β-ENaC abundance was decreased in the cortex/OSOM compared with controls. The γ-ENaC underwent a complex change associated with the increased abundance of the 70-kD band with a concomitant decrease in the main 85-kD band (Figure 3). In contrast, there were no significant changes of abundance of ENaC subunits in group B (Figure 3).

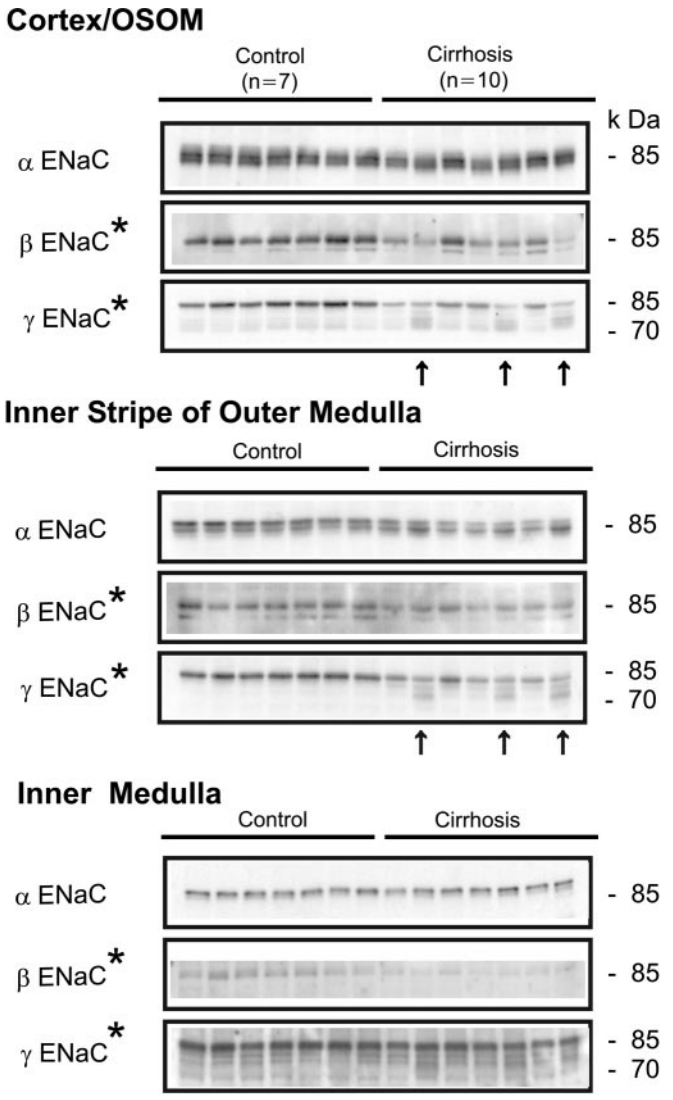

Figure 2. Semiquantitative immunoblots of kidney protein prepared from cortex/outer stripe of outer medulla (OSOM), inner stripe of outer medulla (ISOM), and inner medulla from control rats and CCl_4-treated rats with cirrhosis in protocol 1. The α subunit of the epithelial sodium channel (α-ENaC) band at 85 kD was maintained, and the β-ENaC band at 85 kD was decreased in the cortex/OSOM, ISOM, and inner medulla. The γ-ENaC underwent a complex change. These perturbations were associated with the appearance of a 70-kD band with a concomitant decrease in the main 85-kD band. These changes were prominent, especially in the CCl_4-treated rats associated with markedly decreased urinary sodium excretion (arrows indicate the group 1 rats). *$P < 0.05$ *versus* control.

Increased Apical Targeting of ENaC Subunits in Liver Cirrhosis (Group A, Protocol 1)

To investigate whether the trafficking of ENaC subunits is altered in CCl_4-treated rats, we carried out immunoperoxidase microscopy of ENaC subunits. According to the light microscopic findings, we can differentiate the tubular segmental distributions. The distal convoluted tubule (DCT) cells contain numerous mitochondria in the cytoplasm and the nuclei that

Table 2. Densitometric analysis of ENaC expression (12-wk experiment, protocol 1)[a]

	Control ($n = 7$)	Cirrhosis ($n = 10$)
Cortex/OSOM		
α-ENaC	100 ± 4%	98 ± 4%
β-ENaC	100 ± 10%	50 ± 11%[b]
γ-ENaC 85 kD	100 ± 9%	38 ± 6%[b]
γ-ENaC 70 kD	100 ± 11%	171 ± 77%
ISOM		
α-ENaC	100 ± 8%	82 ± 10%
β-ENaC	100 ± 22%	41 ± 10%[b]
γ-ENaC 85 kD	100 ± 6%	64 ± 5%[b]
γ-ENaC 70 kD	100 ± 22%	428 ± 156%[b]
Inner medulla		
α-ENaC	100 ± 4%	99 ± 7%
β-ENaC	100 ± 17%	24 ± 16%[b]
γ-ENaC 85 kD	100 ± 5%	73 ± 10%[b]
γ-ENaC 70 kD	100 ± 9%	123 ± 28%

[a]Values are expressed as mean ± SE. ENaC, epithelial sodium channel; OSOM, outer stripe of the outer medulla; ISOM, inner stripe of the inner medulla.
[b]$P < 0.05$ *versus* control.

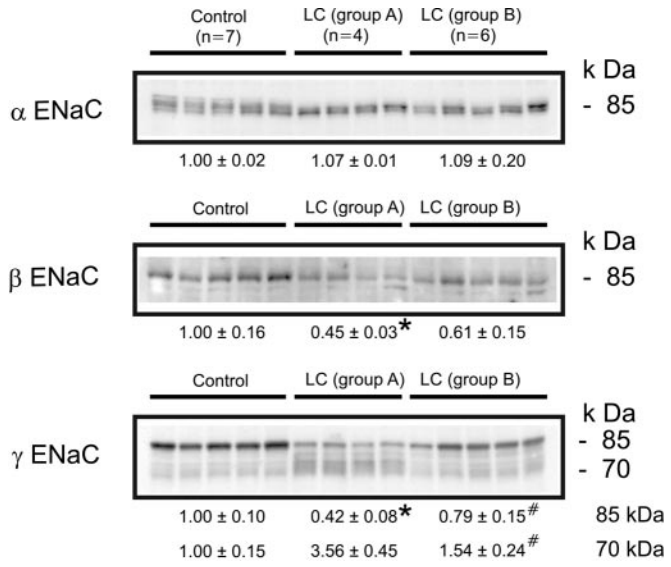

Figure 3. Semiquantitative immunoblots of kidney protein prepared from cortex/OSOM of control and CCl_4-treated rats with cirrhosis subdivided into group A or group B liver cirrhosis in protocol 1. In group A, protein abundance of α-ENaC was unchanged, whereas β-ENaC abundance was decreased compared with controls. The γ-ENaC underwent a complex change associated with the increased abundance of the 70-kD band with a concomitant decrease in the main 85-kD band. In contrast, there were no significant changes of ENaC subunit expression in group 2. *$P < 0.05$ *versus* control; #$P < 0.05$ *versus* group 1.

occupy middle to apical position. The connecting tubule (CNT) cells are intermediate in ultrastructure between the DCT and the collecting duct principal cell. They are taller than principal cells of collecting duct. DCT and CNT are located in the cortical labyrinth. Collecting duct principal cells in the cortex are cuboidal in rats. They have a simple cell shape with light-staining cytoplasm, with fairly straight lateral cell borders, and nucleus is situated in the upper half of the cell in the cortex. The cortical collecting duct (CCD) can be subdivided further into two parts: Initial CCD in the cortical labyrinth and the collecting duct located in the medullary ray. We have examined the CCD in the medullary ray only because initial CCD was not easy to distinguish from CNT in the cortical labyrinth. To confirm the tubule segments, double labeling with γ-ENaC and calbindin-D28k (a marker for DCT and CNT segments) was carried out and analyzed by laser scanning confocal microscopy, as described previously in detail (24).

In control rats, immunoperoxidase staining for the γ-ENaC subunits showed diffuse cytoplasmic labeling throughout the DCT, CNT, and collecting duct principal cells (Figure 4, A, D, G, and J). In contrast, rats in group A of liver cirrhosis revealed γ-ENaC labeling predominantly localized to the apical plasma

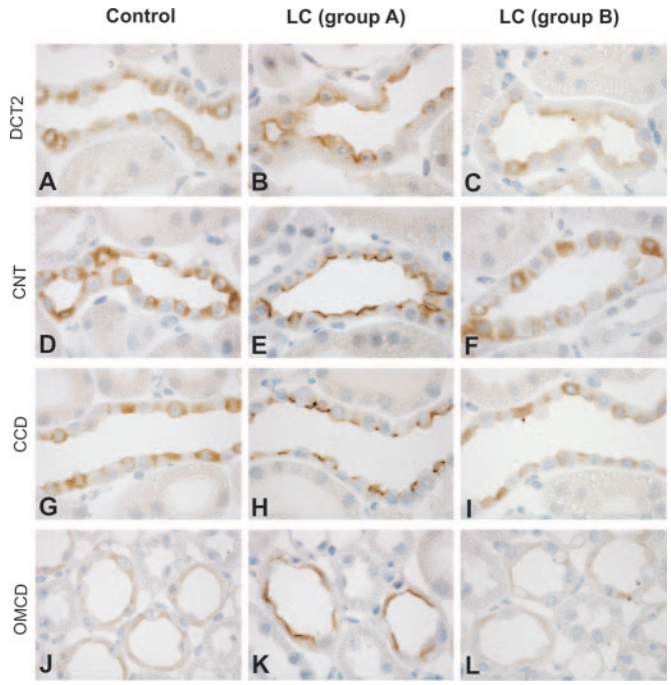

Figure 4. Immunoperoxidase microscopy of γ-ENaC in the second half of distal convoluted tubule (DCT2), connecting tubule (CNT), cortical collecting duct (CCD), and outer medullary collecting duct (OMCD) in protocol 1. Immunoperoxidase labeling of γ-ENaC is dispersed in the cytoplasm of principal cells of the DCT2 (A), CNT (D), CCD (G), and OMCD (J) in control rats. In contrast, γ-ENaC labeling was seen predominantly localized to the apical plasma membrane domains, and only marginal cytoplasmic labeling was observed in DCT2 (B), CNT (E), CCD (H), and OMCD (K) in group A. However, the immunolabeling pattern of γ-ENaC was similar in group B liver cirrhosis compared with controls.

membrane domains with weaker cytoplasmic labeling. This was evident in all of the cross-sectioned tubules of DCT2 (Figure 4B), CNT (Figure 4E), CCD (Figure 4H), and outer medullary collecting duct (OMCD; Figure 4K). On the contrary, rats in group B of liver cirrhosis had a similar immunolabeling pattern of γ-ENaC (Figure 4, C, F, I, and L) to the control rats (Figure 4, A, D, G, and J).

Immunohistochemical analysis also revealed changes in the subcellular redistribution of β-ENaC in kidneys from CCl_4-treated rats similar to the changes of γ-ENaC. There was a marked increase in apical β-ENaC immunolabeling in DCT2 (Figure 5B), CNT (Figure 5E), CCD (Figure 5H), and OMCD (Figure 5K) in kidneys from group A. In contrast, the immunolabeling pattern of β-ENaC in group B (Figure 5, C, F, I, and L) was unchanged (Figure 5, A, D, G, and J). Consistently, immunoperoxidase microscopy revealed an increased apical immunolabeling of α-ENaC in DCT2 (Figure 6B), CNT (Figure 6E), CCD (Figure 6H), and OMCD (Figure 6K) in group A but not in group B (Figure 6, C, F, I, and L).

Changes of Urinary Sodium Excretion in CCl_4-Treated Rats (11-Wk Experiment, Protocol 2)

Table 4 shows the changes in liver and renal function in protocol 2 (11-wk experiment). All of the CCl_4-treated rats had significant amount of ascites. Plasma concentrations of ALT and bilirubin were significantly increased in CCl_4-treated rats. Plasma creatinine and renal creatinine clearance were not changed in CCl_4-treated rats. The 24-h urinary sodium excretion and fractional excretion of sodium were decreased, and accordingly sodium balance was positive in CCl_4-treated rats (Table 4).

In protocol 2 of 11 wk of CCl_4 treatment, we subdivided CCl_4-treated rats into two groups (group A and group B) according to the urinary sodium excretion, similar to protocol 1. Four rats (group A) out of all of the CCl_4-treated rats showed markedly decreased urinary sodium excretion and urinary Na/K ratio compared with controls, whereas the other seven rats (group B) had unchanged urinary sodium excretion and Na/K ratio (Table 5). In contrast to protocol 1, plasma aldosterone levels were not changed in group A. The levels were decreased in group B compared with controls (Table 5).

Altered Regulation of ENaC Abundance and Trafficking (11-Wk Experiment, Protocol 2)

In protocol 2, the major changes of abundance and subcellular distribution of ENaC subunits were virtually identical to those of protocol 1. The protein abundance of α-ENaC and β-ENaC was unchanged. However, the γ-ENaC underwent a

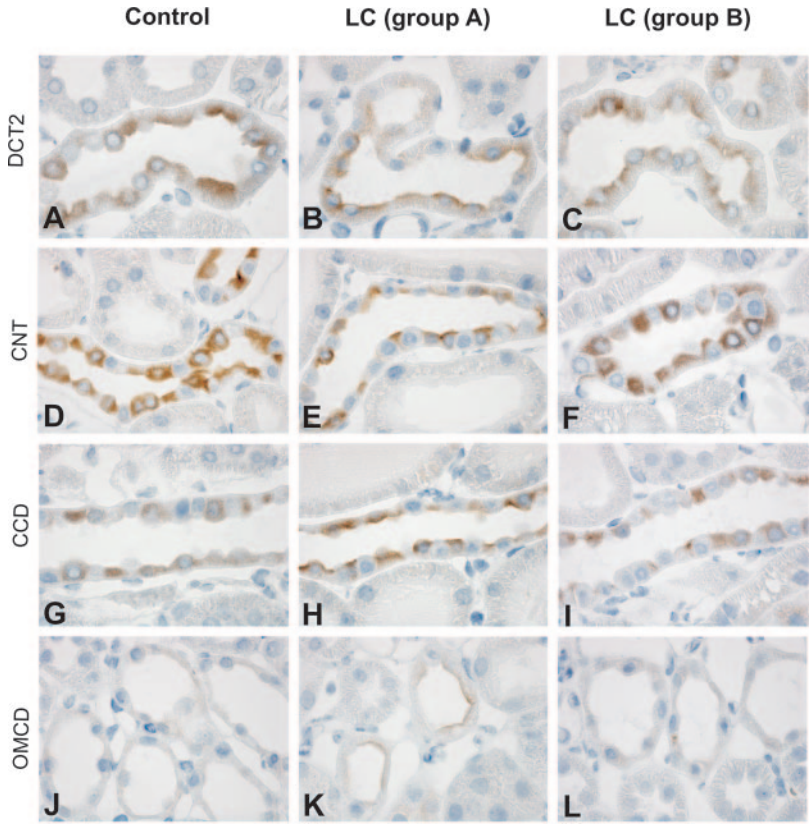

Figure 5. Immunoperoxidase microscopy of β-ENaC in DCT2, CNT, CCD, and OMCD in protocol 1. Immunoperoxidase labeling of β-ENaC is associated mainly with the entire cytoplasm of principal cells of the DCT2 (A), CNT (D), CCD (G), and OMCD (J) in control rats. In contrast, β-ENaC labeling was markedly redistributed to the apical plasma membrane domains in DCT2 (B), CNT (E), CCD (H), and OMCD (K) in group A cirrhosis. However, the immunolabeling pattern of β-ENaC was similar in group B liver cirrhosis compared with controls.

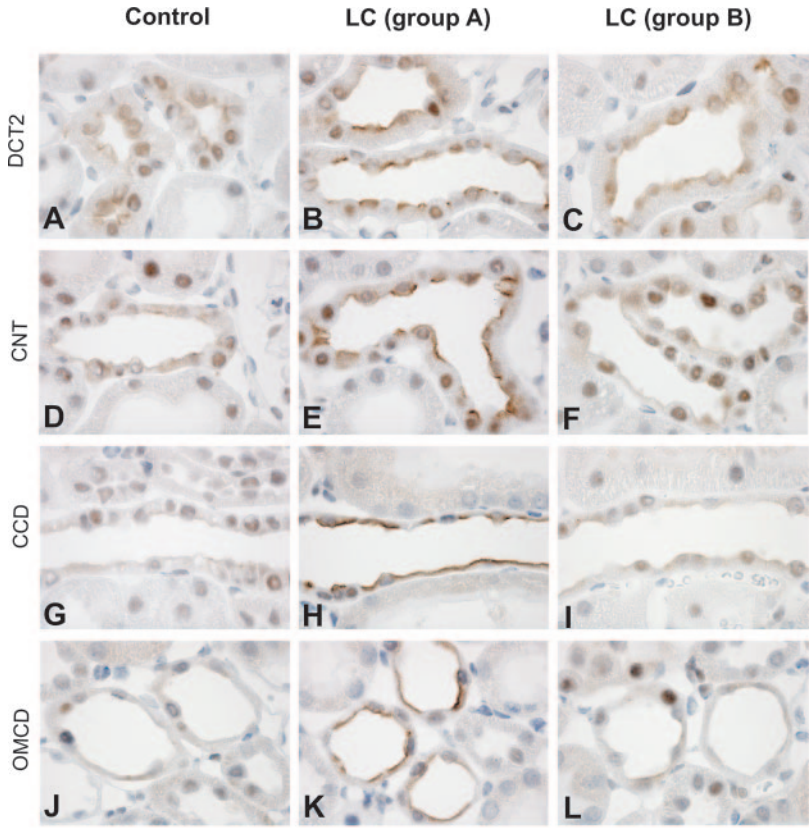

Figure 6. Immunoperoxidase microscopy of α-ENaC in DCT2, CNT, CCD, and OMCD in protocol 1. Immunoperoxidase labeling of α-ENaC is restricted to a narrow zone in the apical part, including the plasma membrane domains of the principal cells of the DCT2 (A), CNT (D), CCD (G), and OMCD (J) in control rats. In contrast, group A rats with cirrhosis showed markedly increased apical immunolabeling of α-ENaC in DCT2 (B), CNT (E), CCD (H), and OMCD (K). However, the immunolabeling pattern of α-ENaC was similar in group B liver cirrhosis compared with controls.

Table 3. Subgroup analysis of urinary sodium excretion and plasma aldosterone levels (12-wk experiment, protocol 1)[a]

	Control ($n = 7$)	Group A ($n = 4$)	Group B ($n = 6$)
$U_{Na} \times UO$ (mmol)	1.45 ± 0.12	0.12±0.05[b]	1.53 ± 0.48[c]
FE_{Na} (%)	0.50 ± 0.12	0.07 ± 0.01[b]	0.50 ± 0.05[c]
FE_K (%)	33.7 ± 2.1	31.4 ± 9.0	35.6 ± 6.5
Urine Na/K	0.36 ± 0.02	0.05 ± 0.01[b]	0.33 ± 0.03[c]
P_{aldo} (pg/ml)	203.6 ± 35.0	1064.3 ± 235.0[b]	76.0 ± 20.0[c,d]

[a]Values are expressed as mean ± SE. These values are measured at the last day of experiments (12 wk).
[b]$P < 0.01$ *versus* control.
[c]$P < 0.01$ *versus* group A.
[d]$P < 0.05$ *versus* control.

complex change associated with the increased abundance of the 70-kD band with a concomitant decrease in the main 85-kD band in group A but not in group B (Figure 7A). There was a prominent increase in apical trafficking of β-ENaC and γ-ENaC in DCT2, CNT, CCD, and OMCD in group A but not in group B. Representative immunoperoxidase labeling of γ-ENaC in the CCD showed an increased apical labeling in group A, whereas no change of subcellular distribution of γ-ENaC was observed in group B compared with controls (Figure 7B).

Decreased Protein Abundance of 11βHSD2 in CCl_4-Treated Rats

Semiquantitative immunoblotting was carried out to investigate whether the abundance of 11βHSD2 was altered in rats with CCl_4-induced liver cirrhosis. In protocol 1, the protein abundance of 11βHSD2 was decreased in the cortex/OSOM (51 ± 8 *versus* 100 ± 16% in controls; $P < 0.05$; Figure 8A) but not changed in ISOM (93 ± 6 *versus* 100 ± 5% in controls; NS) and inner medulla (138 ± 41 *versus* 100 ± 23% in controls; NS).

Table 4. Changes in liver and renal function (11-wk experiment, protocol 2)[a]

	Control ($n = 7$)	Cirrhosis ($n = 11$)
Body weight (g)	306.4 ± 2.8	306.9 ± 7.3
Ascites (ml)	Nondetectable	7.3 ± 1.6
UO (μl/min)	9.1 ± 0.6	7.8 ± 0.6
P_{ALT} (U/L)	42.8 ± 2.2	185.6 ± 28.4[b]
$P_{bilirubin}$ (μmol/L)	2.0 ± 0.2	6.9 ± 1.5[b]
Pcr (μmol/L)	32.3 ± 2.3	29.2 ± 3.3
Ccr (ml/min)	1.47 ± 0.09	1.40 ± 0.12
P_{Na} (mEq/L)	137.8 ± 0.6	136.7 ± 0.2
P_K (mEq/L)	4.4 ± 0.1	4.7 ± 0.1
U_{Na}×UO (mmol)	1.88 ± 0.06	1.24 ± 0.18[c]
Na balance (mmol/d)	0.02 ± 0.05	0.52 ± 0.27[c]
FE_{Na} (%)	0.66 ± 0.05	0.49 ± 0.07[c]
FE_K (%)	45.3 ± 2.6	44.0 ± 2.7
Urine Na/K	0.45 ± 0.01	0.34 ± 0.05[c]

[a]Values are expressed as mean ± SE. These values are measured at the last day of experiments (11 wk).
[b]$P < 0.01$ *versus* control.
[c]$P < 0.05$ *versus* control.

To investigate whether there were changes in the protein abundance and/or immunolabeling of 11βHSD2 among group A and group B of liver cirrhosis and controls, we performed additional immunoblotting and immunocytochemical analysis. Compared with controls, the abundance of 11βHSD2 was markedly decreased in the cortex/OSOM in group A from both protocols (Figure 8, B [protocol 1] and C [protocol 2]) but not in group B. Immunolabeling of 11βHSD2 was associated with DCT2, CNT, and collecting duct principal cells. Immunoperoxidase microscopy revealed cytoplasmic staining of 11βHSD2 that was observed mainly at the perinuclear region (Figure 9). However, immunogold electron microscopy for 11βHSD2 in the kidney of control rats revealed that immunogold labeling was diffusely distributed to whole cytoplasm and was not concentrated to the perinuclear region (data not shown). Importantly, rats in group A from protocol 1 demonstrated decreased immunolabeling intensity of 11βHSD2 in DCT2 (Figure 9B), CNT (Figure 9E), and CCD (Figure 9H). In contrast, rats in group B from protocol 1 did not reveal any significant changes of the immunolabeling of 11βHSD2 in the DCT2 (Figure 9C), CNT (Figure 9F), and CCD (Figure 9I), compared with control rats (Figure 9, A, D, and G). In contrast, immunolabeling intensity of 11βHSD2 in OMCD did not show any significant changes among the three groups (Figure 9, J, K, and L).

Altered Protein Abundance of Major Renal Sodium Transporters in CCl_4-Treated Rats (12-Wk Experiment, Protocol 1)

Protein abundance of the α1-isoform of Na,K-ATPase was unchanged in the cortex/OSOM, ISOM, and inner medulla (Table 6). The NHE3 abundance was decreased in the cortex/OSOM but was increased in the ISOM (Figure 10, Table 6). Immunocytochemistry demonstrated that the labeling intensity of NHE3 in the proximal tubule of CCl_4-treated kidney was reduced but was increased in medullary thick ascending limb (mTAL) compared with control rats (data not shown). The protein abundance of NKCC2 was increased in ISOM (Figure 10) in CCl_4-treated rats but was not altered in the cortex/OSOM (Table 6). In contrast to the significant changes in renal protein abundance of NHE3 and NKCC2, the NCC abundance was unchanged in the cortex/OSOM (Table 6).

Increased Protein Abundance and Apical Plasma Membrane Targeting of AQP2 and p-AQP2 in CCl_4-Treated Rats (12-Wk Experiment, Protocol 1)

Semiquantitative immunoblotting revealed an increase in AQP2 abundance in the inner medulla (221 ± 21 *versus* 100 ± 14% in controls; $P < 0.05$; Figure 11, A and B), whereas there were no changes in the cortex/OSOM (115 ± 10 *versus* 100 ± 15% in controls; NS) and ISOM (114 ± 6 *versus* 100 ± 9%; NS). Moreover, semiquantitative immunoblotting with antibodies that selectively recognize AQP2 (p-AQP2), which is phosphorylated in the protein kinase A phosphorylation consensus site (Ser256) (25), demonstrated that the abundance of p-AQP2 was also increased in the inner medulla (198 ± 28 *versus* 100 ± 15%; $P < 0.05$) but was not changed in the cortex/OSOM (100 ± 7 *versus* 100 ± 9%; NS) and ISOM (98 ± 7 *versus* 100 ± 15%; NS).

The changes in trafficking of AQP2 and p-AQP2 were examined by immunoperoxidase microscopy. Immunolabeling of AQP2 was seen exclusively in collecting duct principal cells. There was a prominent difference in the subcellular localization of AQP2 in kidneys from CCl_4-treated and control rats in the inner medullary collecting duct. In CCl_4-treated rats, AQP2 labeling was mainly associated with the apical plasma membrane domains with weaker labeling intensity of cytoplasmic domains (Figure 11D). In contrast, AQP2 labeling in kidneys of control rats showed weaker labeling intensity throughout the cytoplasm with less prominent apical plasma membrane labeling (Figure 11C). Immunohistochemistry also revealed similar changes in the subcellular distribution of p-AQP2 in kidney from CCl_4-treated rats. There was a marked increase in apical p-AQP2 immunolabeling in CCl_4-treated rats (Figure 11F) compared with control rats (Figure 11E).

Discussion

This study was undertaken to elucidate renal mechanisms in the disturbed sodium metabolism in rats with decompensated liver cirrhosis induced by chronic administration of CCl_4. The renal responses for sodium retention displayed wide variations among the rats with liver cirrhosis. Some rats showed markedly decreased urinary sodium excretion (sodium retaining stage, group A), whereas the others exhibited unchanged urinary sodium excretion (maintenance stage, group B) compared with controls, even though all CCl_4-treated rats had a significant amount of ascites. The results demonstrated that CCl_4-induced sodium retaining stage (group A) of liver cirrhosis was associated with (*1*) decreased urinary sodium excretion and increased or maintained plasma aldosterone levels; (*2*) increased apical

Table 5. Subgroup analysis of urinary sodium excretion and plasma aldosterone levels (11-wk experiment, protocol 2)[a]

	Control ($n = 7$)	Group A ($n = 4$)	Group B ($n = 7$)
$U_{Na} \times UO$ (mmol)	1.88 ± 0.06	0.59 ± 0.09[b]	1.61 ± 0.14[c]
FE_{Na} (%)	0.66 ± 0.05	0.20 ± 0.05[b]	0.65 ± 0.03[c]
FE_K (%)	45.3 ± 2.6	47.2 ± 4.6	42.2 ± 3.4
Urine Na/K	0.45 ± 0.01	0.12 ± 0.02[b]	0.46 ± 0.02[c]
P_{aldo} (pg/ml)	467.3 ± 46.0	462.0 ± 96.0	271.8 ± 45.0[d]

[a]Values are expressed as mean ± SE. These values are measured at the last day of experiments (12 wk).
[b]$P < 0.01$ *versus* control.
[c]$P < 0.01$ *versus* group A.
[d]$P < 0.05$ *versus* control.

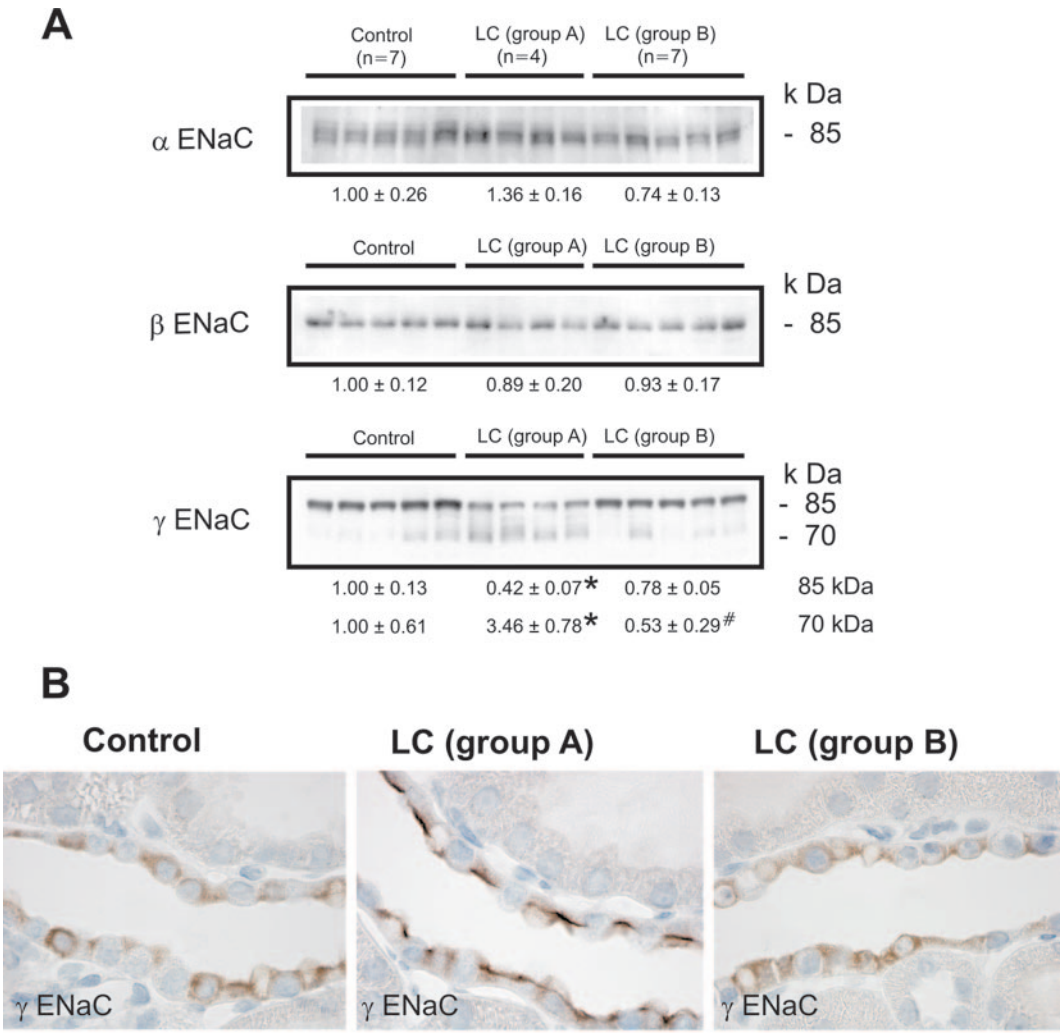

Figure 7. Semiquantitative immunoblots (A) and immunoperoxidase microscopy (B) of ENaC subunits prepared from cortex/OSOM of control and CCl_4-treated rats with cirrhosis (11 wk) in protocol 2. (A) In group A, protein abundance of α-ENaC and β-ENaC was unchanged compared with controls, whereas γ-ENaC underwent a complex change associated with the increased abundance of the 70-kD band with a concomitant decrease in the main 85-kD band. There were no significant changes of ENaC subunit expression in group B. (B) Immunoperoxidase labeling of γ-ENaC is dispersed in the cytoplasm of principal cells of the CCD in control rats. The labeling is markedly increased in the apical plasma membrane domains in group A, whereas the subcellular distribution of γ-ENaC was similar in group B liver cirrhosis compared with controls. *$P < 0.05$ *versus* control; #$P < 0.05$ *versus* group A.

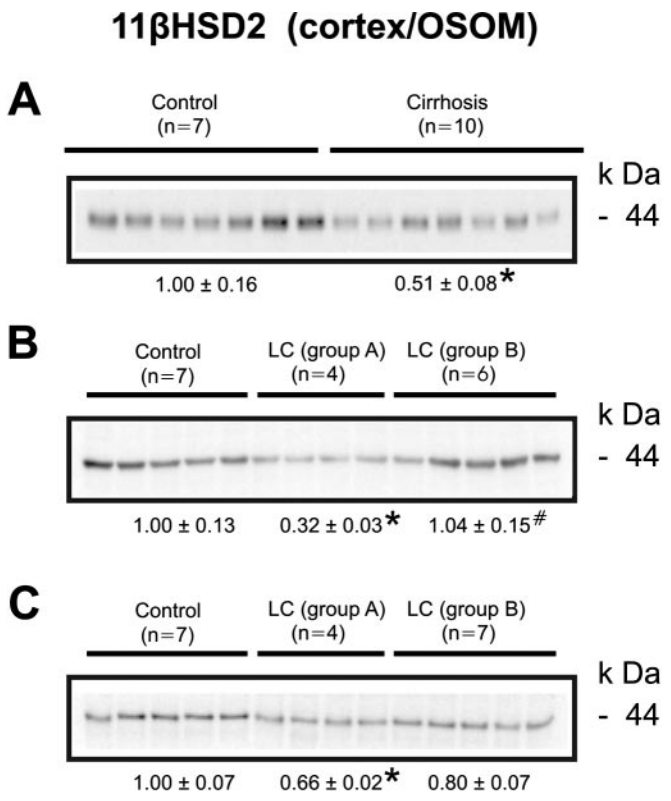

Figure 8. Semiquantitative immunoblotting of the type 2 isoform of 11β-hydroxysteroid dehydrogenase (11βHSD2) from cortex/OSOM in protocol 1 (A and B) and protocol 2 (C). (A) Protein abundance of 11βHSD2 in the cortex/OSOM was significantly reduced in CCl_4-treated rats compared with control rats (12 wk). (B) Compared with controls, the abundance of 11βHSD2 was markedly decreased in cortex/OSOM in group A but not in group B compared with controls (12 wk). (C) Similar changes were observed in 11-wk CCl_4-treated rats with cirrhosis. The 11βHSD2 expression was markedly decreased in cortex/OSOM in group A but not in group B. *$P < 0.05$ *versus* control.

targeting of ENaC subunits in DCT2, CNT and collecting duct segments; and (3) decreased protein abundance of 11βHSD2. In contrast, maintenance stage (group B) of liver cirrhosis was associated with no changes in the urinary sodium excretion, trafficking, and abundance of ENaC subunits and the abundance of 11βHSD2.

Increased Apical Targeting of ENaC Subunits in CCl_4-Treated Rats

In this study, the most important finding is the striking increase in targeting of all ENaC subunits to the apical plasma membrane domain in DCT2, CNT, and collecting duct in the sodium-retaining stage (group A) but not in the maintenance stage (group B) of liver cirrhosis. Because an increased targeting of all ENaC subunits to the apical plasma membrane is associated with increased sodium reabsorption, our finding of an increased ENaC targeting in the sodium-retaining stage of liver cirrhosis could contribute significantly to the increased renal tubular sodium reabsorption. These observations therefore strongly support the view that the renal sodium retention in the decompensated liver cirrhosis is caused mainly by an increased sodium reabsorption in distal nephron, including the collecting duct (6). It is noteworthy that the experimental animals are slightly hyponatremic relative to the controls. Thus, water retention seems to exceed the sodium retention. Consistent with this, the changes in AQP2 all are consistent with increased vasopressin levels (2,23). Arguably, this means that the sodium retention is appropriate to retain plasma osmolality.

Altered Protein Abundance of ENaC Subunits in CCl_4-Treated Rats

We demonstrated that the abundance of β-ENaC was decreased or unchanged and the abundance of the 70-kD form of γ-ENaC was increased whereas the 85-kD band was markedly decreased in the sodium-retaining stage (group A) of rats with cirrhosis rats. Previous studies demonstrated that aldosterone causes a mobility shift of γ-ENaC from an 85- to a 70-kD band without a change in total γ-ENaC protein abundance (13). The appearance of the 70-kD form of γ-ENaC in response to aldosterone is putatively due to a channel-activating proteolytic cleavage (27). The same changes are observed in chronically sodium-restricted rats in addition to a significant downregulation of the β-ENaC subunit (13). Thus, the observed increased apical targeting and altered expression of β- and γ-ENaC subunits in group A could be caused by the stimulation of MR in the aldosterone-responsive epithelium.

Recent studies demonstrated that the abundance of NCC and α-ENaC are increased by aldosterone treatment in normal rats (13,28). In contrast, in our study we did not observe any changes of the abundance of NCC and α-ENaC in CCl_4-induced liver cirrhosis, where plasma aldosterone levels were elevated. Consistent with this, we previously demonstrated that puromycin aminonucleoside–induced nephrotic syndrome was associated with an increased apical targeting of ENaC subunits, but the protein abundance of α-ENaC was not changed in the kidney cortex in the presence of increased plasma aldosterone levels (24). Moreover, we previously demonstrated that α-ENaC abundance was not changed in lithium-treated rats, in which plasma aldosterone levels were significantly increased (29). In both puromycin aminonucleoside– and lithium-treated rats, apical trafficking of ENaC subunits was markedly increased, whereas NCC abundances were decreased, suggesting that changes of trafficking of ENaC subunits and abundance of aldosterone-sensitive transporters (α-ENaC and NCC) are dissociated in pathophysiologic conditions. Moreover, mineralocorticoid activity can be regulated by different mechanisms: At the prereceptor level (*e.g.*, 11βHSD2), at the receptor level, and at the postreceptor level of transcriptional activation or repression by cell-specific co-factors (30). Each of these cellular events ultimately will influence the nature and/or the magnitude of the response of the tissue after the stimulation of MR. Thus, it can be speculated that other factors that are at least as effective as aldosterone in modulating ENaC expression/trafficking play a role, or probably the interaction of MR is modified by some local factors in experimental liver cirrhosis.

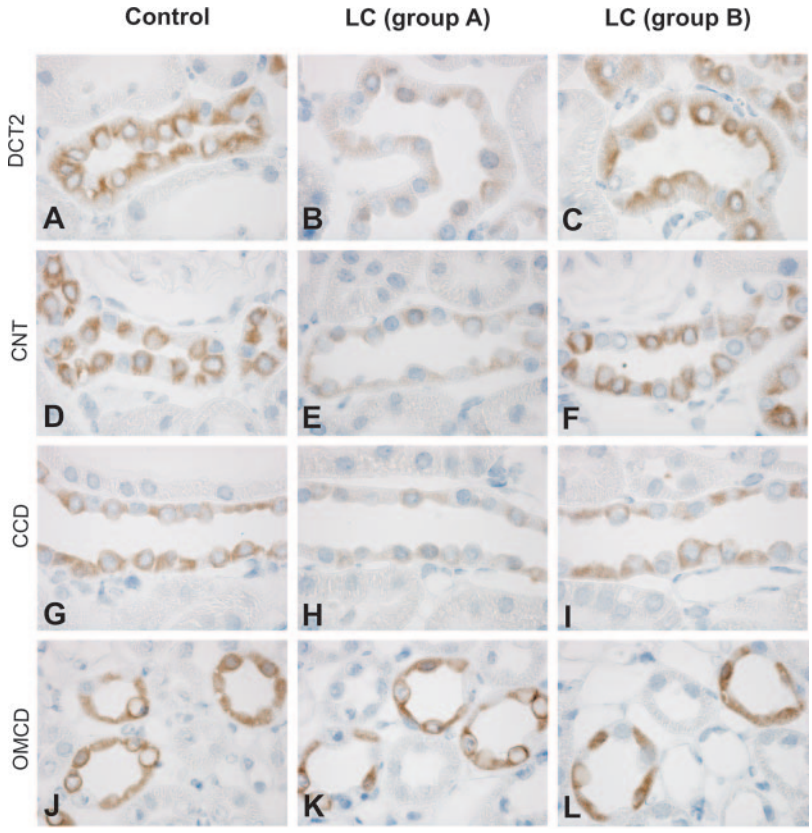

Figure 9. Immunoperoxidase microscopy of 11βHSD2 in DCT2, CNT, CCD, and OMCD in protocol 1. Immunoperoxidase labeling of 11βHSD2 was dispersed in the cytoplasm of principal cells of the DCT2 (A), CNT (D), CCD (G), and OMCD (J) in control rats. In group A rats with cirrhosis, the immunolabeling intensity of 11βHSD2 was markedly decreased in DCT2 (B), CNT (E), and CCD (H). However, group B rats with liver cirrhosis did not show any significant changes of the immunolabeling intensity in the DCT2 (A and C), CNT (D and F), and CCD (G and I) compared with control rats. Immunolabeling intensity of 11βHSD2 in OMCD did not show any significant changes among three groups (J, K, and L).

Decreased Urinary Na/K Ratio in Group A but not in Group B of Liver Cirrhosis

The urinary Na/K ratio has widely been used to evaluate aldosterone activity at the distal nephron and collecting duct (31,32). Accordingly, the sodium-retaining stage (group A rats with cirrhosis) in both protocols 1 and 2 was associated with markedly decreased urinary Na/K ratio, indicating an increased aldosterone effect in the distal nephron. In contrast, maintenance stage (group B rats with cirrhosis) in protocols 1 and 2 was associated with unchanged Na/K ratio and marginally decreased plasma aldosterone levels. This may play a compensatory role to promote the urinary sodium excretion in this stage of liver cirrhosis. Thus, dynamic changes of circulating aldosterone levels could play a role in the sodium retention in liver cirrhosis.

At the initial stage of decompensated cirrhosis, in which the renin-angiotensin-aldosterone system (RAAS) and sympathetic nervous system are usually not activated, sodium retention could be due to mechanisms that are unrelated to arterial vascular underfilling and increased plasma aldosterone levels (33,34). This would correspond to what we observed in 11 wk protocol. Circulatory dysfunction at this phase, although greater than in compensated cirrhosis without ascites, is not intense enough to stimulate the RAAS (35). However, previous studies on the intrarenal sodium handling strongly indicate that sodium retention observed in this stage occurs predominantly at the aldosterone-sensitive distal nephron (7). Thus, in addition to the action of aldosterone itself, other possible mechanisms contributing to the activation of MR at the distal nephron should be considered. As disease progresses, an activation of RAAS and sympathetic nervous system could also be involved in the pathogenesis of sodium retention later on, and this results in a more severe impairment in the sodium and water balance (33,34). In this study, we demonstrated that in the sodium-retaining stage (group A) of liver cirrhosis, an increased urinary sodium reabsorption was associated with the markedly increased apical targeting of ENaC subunits as well as decreased urinary Na/K ratio with maintained (11-wk experiment) or increased (12-wk experiment) plasma aldosterone levels. These differences may verify that the pathophysiologic state reached in the two phases is different even though both are associated with sodium retention.

Table 6. Densitometric analysis of sodium transporter expression (12-wk experiment, protocol 1)[a]

	Control ($n = 7$)	Cirrhosis ($n = 10$)
Cortex/OSOM		
Na,K-ATPase α1	100 ± 19%	145 ± 10%
NHE3	100 ± 9%	71 ± 4%[b]
NKCC2	100 ± 19%	138 ± 22%
NCC	100 ± 19%	145 ± 15%
ISOM		
Na,K-ATPase α1	100 ± 15%	126 ± 19%
NHE3	100 ± 10%	174 ± 16%[b]
NKCC2	100 ± 15%	179 ± 16%[b]
Inner medulla		
Na,K-ATPase α1	100 ± 7%	89 ± 6%

[a]Values are expressed as mean ± SE. NHE3, type 3 Na/H exchanger; NKCC2, Na-K-2Cl co-transporter; NCC, thiazide-sensitive Na-Cl co-transporter.
[b]$P < 0.05$ compared with control.

Decreased Protein Abundance and Immunolabeling Intensity of 11βHSD2 in CCl_4-Treated Rats with Sodium Retention

We also demonstrated that there is a downregulation of 11βHSD2 in renal cortex/OSOM. This finding is consistent with recent studies that demonstrated decreased 11βHSD2 activity in the kidneys of liver cirrhosis induced by bile duct obstruction (35,36). These findings suggest that reduced activity of 11βHSD2 provides unhindered access of glucocorticoids to the MR, resulting in the increased aldosterone effectiveness and renal sodium retention. In this study, we demonstrated that an increased apical targeting of ENaC subunits was associated with the decreased protein abundance of 11βHSD2 in the sodium-retaining stage of liver cirrhosis (group A) in both protocols 1 and 2, in which urinary sodium excretion was markedly decreased. Furthermore, a mobility shift of γ-ENaC from an 85 to a 70-kD band, a representative finding of aldosterone effect, was also associated with decreased 11βHSD2 abundance. Thus, increased apical targeting and changes of ENaC abundance may be attributed partly to the increased MR activity caused by decreased abundance of 11βHSD2.

Plasma aldosterone levels have been shown to be reduced in conditions with low expression of 11βHSD2 in normal human or rat (21,37). In our study, however, plasma aldosterone levels were not reduced in the sodium-retaining stage of liver cirrhosis (group 1) despite that the protein abundance of 11βHSD2 was significantly decreased. Thus, coordinated activation of the MR by both glucocorticoid as a consequence of reduced activity of 11βHSD2 and increased plasma aldosterone level may stimulate the distal renal tubular sodium reabsorption and potassium loss.

Increased Abundances of NHE3 and NKCC2 in ISOM from CCl_4-Treated Rats

It has been demonstrated that rats with common bile duct ligation–induced liver cirrhosis had an increased natriuretic response to furosemide together with marked hypertrophy of the mTAL cells in the ISOM (38,39). During the later decompensated stage, in which the renal sympathetic nerves and the RAAS are activated, cirrhosis is associated with avid sodium retention and edema. Concomitant increase of plasma vasopressin, glucagon, and insulin also contribute to the stimulation of sodium reabsorption in the mTAL in rats with cirrhosis

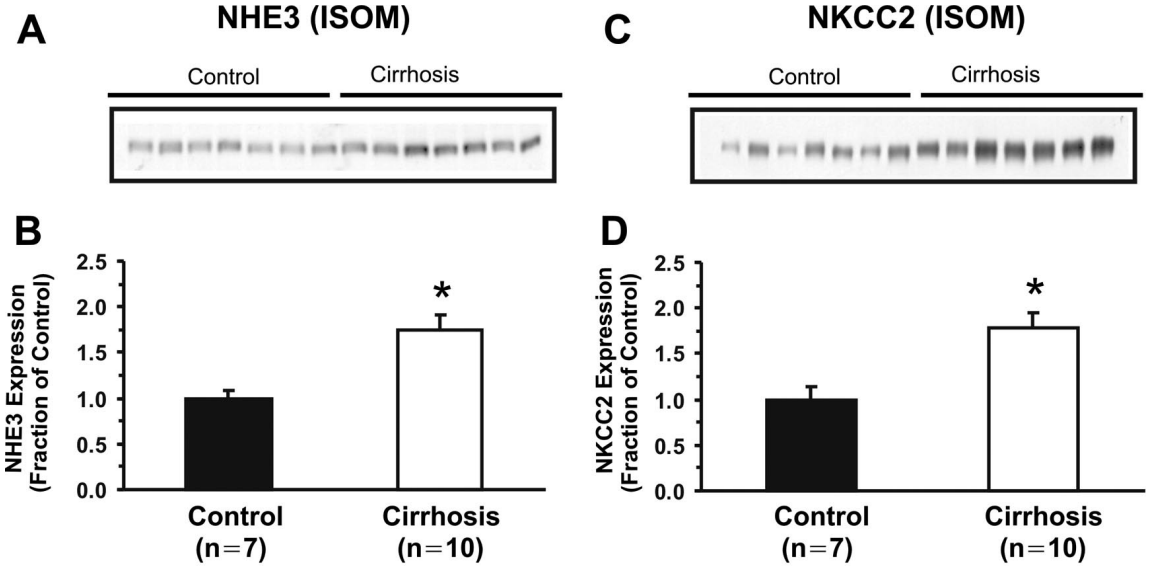

Figure 10. Semiquantitative immunoblotting of kidney protein prepared from ISOM of control and CCl_4-treated rats with cirrhosis in protocol 1. (A) Immunoblot was reacted with anti–type 3 Na/H exchanger (NHE3) antibodies. (B) Densitometric analyses revealed that NHE3 expression in ISOM was increased in CCl_4-treated rats compared with control rats. (C) Immunoblots were reacted with anti–Na-K-2Cl co-transporter (NKCC2) antibodies. (D) Densitometric analyses revealed that NKCC2 expression in ISOM was increased in CCl_4-treated rats compared with control rats. *$P < 0.05$ *versus* control.

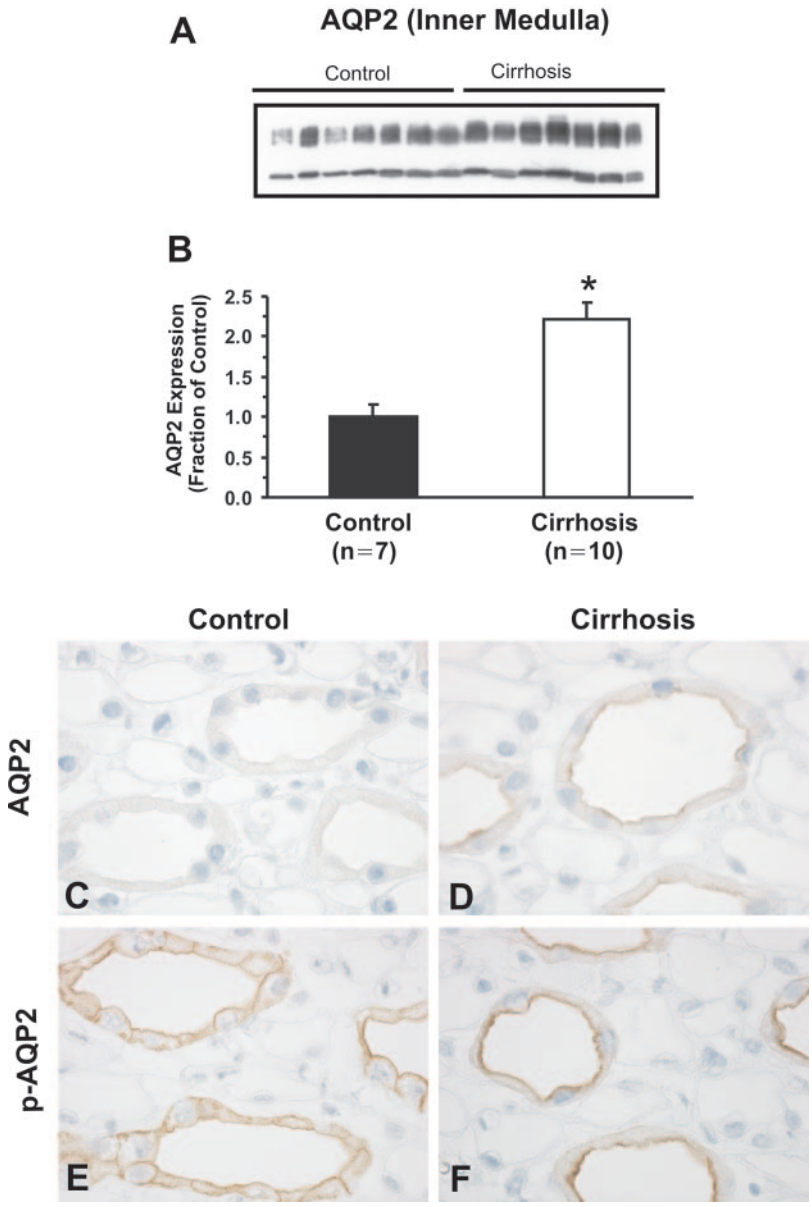

Figure 11. Semiquantitative immunoblotting and immunoperoxidase microscopy of kidney protein prepared from inner medulla of control and CCl_4-treated rats with cirrhosis in protocol 1. (A) Immunoblot was reacted with anti–aquaporin-2 (AQP2) antibodies. (B) Densitometric analyses revealed that AQP2 expression in inner medulla was increased in CCl_4-treated rats compared with control rats. (C and D) Inner medullary collecting duct (IMCD) from control rats showed diffuse cytoplasmic labeling of AQP2 with less prominent apical plasma membrane labeling, whereas IMCD from CCl_4-treated rats with cirrhosis exhibited AQP2 labeling that was localized mainly to the apical plasma membrane domains with marginal labeling of cytoplasm. (E and F) Immunocytochemical analyses revealed similar changes in the subcellular distribution of phosphorylated-AQP2 (p-AQP2) in kidney from CCl_4-treated rats. There was a marked increase in apical p-AQP2 immunolabeling in CCl_4-treated rats (E) compared with control rats (F).

(40–42). In this study, we demonstrated the increased abundance of NHE3 and NKCC2 in the ISOM in CCl4-treated rats. These observations therefore support the view that the increased renal sodium reabsorption associated with the late decompensated stage of cirrhosis is caused partly by the increased sodium reabsorption in mTAL (43). We here suggest that this occurs *via* upregulated protein abundance of NHE3 and NKCC2 in the mTAL.

Increased Protein Abundance and Apical Targeting of AQP2 and p-AQP2

Regarding the involvement of AQP2 in water retention in liver cirrhosis, previous animal studies showed conflicting results. It was demonstrated that CCl_4-induced liver cirrhosis in rats resulted in increased or unchanged expression of AQP2 mRNA and protein (23,44–46). This discrepancy of AQP2 expression among the studies with the CCl_4 model of decompen-

sated liver cirrhosis is not well understood. In the 12-wk experiment of our study, the protein abundance and apical targeting of AQP2 and p-AQP2 were increased in the inner medulla, along with the increased urine osmolality and urine to plasma osmolality ratio in CCl_4-treated rats. In addition, plasma osmolality was significantly decreased and CCl4-treated rats were marginally hyponatremic compared with controls. These findings indicate that upregulation of the vasopressin-regulated water channel AQP2 abundance may contribute to the increased renal water reabsorption in decompensated liver cirrhosis. In accordance with our results, a previous study that used differential centrifugation of kidney protein samples in rats with liver cirrhosis showed evidence for the redistribution of AQP2 to the plasma membrane (46). Consistent with this, urinary AQP2 excretion, which would be attributed to the increased cellular trafficking, was increased in patients with liver cirrhosis (47). Thus, the inconsistent findings of AQP2 abundance in kidneys of animals with liver cirrhosis may reflect the variation of disease severity.

Conclusion

The results demonstrate underlying molecular mechanisms for the disturbed sodium metabolism in rats with decompensated liver cirrhosis induced by chronic administration of CCl_4. Increased apical targeting of ENaC subunits combined with diminished abundance of 11βHSD2 in the DCT2, CNT, and collecting duct is likely to play an additive role in the sodium-retaining stages of liver cirrhosis. The upregulation of the vasopressin-regulated water channel AQP2 as well as increased apical AQP2 targeting is likely to contribute to the increased water reabsorption and urinary concentration in liver cirrhosis.

Acknowledgments

We thank Ida Maria Jalk, Gitte Kall, Helle Høyer, Zhila Nikrozi, Inger Merete Paulsen, Lotte Vallentin Holbech, Mette Vistisen, and Dorte Wulff for expert technical assistance. The Water and Salt Research Center at the University of Aarhus is established and supported by the Danish National Research Foundation (Danmarks Grundforskningsfond). Support for this study was provided by the Karen Elise Jensen Foundation, Human Frontier Science Program; the European Commission (QRLT 2000 00778 and QRLT 2000 00987); the Regional Technology Innovation Program of the MOCIE (RTI04-01-01, T.-H.K.); and the intramural budget of the National Heart, Lung, and Blood Institute, National Institutes of Health.

References

1. Valdivieso A: The kidney in chronic liver disease: Circulatory abnormalities, renal sodium handling and role of natriuretic peptides. *Biol Res* 31: 291–304, 1998
2. Linas SL, Anderson RJ, Guggenheim SJ, Robertson GL, Berl T: Role of vasopressin in impaired water excretion in conscious rats with experimental cirrhosis. *Kidney Int* 20: 173–180, 1981
3. Arroyo V, Bosch J, Mauri M, Viver J, Mas A, Rivera F, Rodes J: Renin, aldosterone and renal haemodynamics in cirrhosis with ascites. *Eur J Clin Invest* 9: 69–73, 1979
4. DiBona GF, Herman PJ, Sawin LL: Neural control of renal function in edema-forming states. *Am J Physiol* 254: R1017–R1024, 1988
5. Jimenez W, Martinez-Pardo A, Arroyo V, Bruix J, Rimola A, Gaya J, Rivera F, Rodes J: Temporal relationship between hyperaldosteronism, sodium retention and ascites formation in rats with experimental cirrhosis. *Hepatology* 5: 245–250, 1985
6. Chaimovitz C, Szylman P, Alroy G, Better OS: Mechanism of increased renal tubular sodium reabsorption in cirrhosis. *Am J Med* 52: 198–202, 1972
7. Angeli P, Gatta A, Caregaro L, Menon F, Sacerdoti D, Merkel C, Rondana M, de Toni R, Ruol A: Tubular site of renal sodium retention in ascitic liver cirrhosis evaluated by lithium clearance. *Eur J Clin Invest* 20: 111–117, 1990
8. Chonko AM, Bay WH, Stein JH, Ferris TF: The role of renin and aldosterone in the salt retention of edema. *Am J Med* 63: 881–889, 1977
9. Rosoff L Jr, Zia P, Reynolds T, Horton R: Studies of renin and aldosterone in cirrhotic patients with ascites. *Gastroenterology* 69: 698–705, 1975
10. Wilkinson SP, Jowett TP, Slater JD, Arroyo V, Moodie H, Williams R: Renal sodium retention in cirrhosis: Relation to aldosterone and nephron site. *Clin Sci* 56: 169–177, 1979
11. Perez-Ayuso RM, Arroyo V, Planas R, Gaya J, Bory F, Rimola A, Rivera F, Rodes J: Randomized comparative study of efficacy of furosemide versus spironolactone in nonazotemic cirrhosis with ascites. Relationship between the diuretic response and the activity of the renin-aldosterone system. *Gastroenterology* 84: 961–968, 1983
12. Duc C, Farman N, Canessa CM, Bonvalet JP, Rossier BC: Cell-specific expression of epithelial sodium channel alpha, beta, and gamma subunits in aldosterone-responsive epithelia from the rat: Localization by in situ hybridization and immunocytochemistry. *J Cell Biol* 127: 1907–1921, 1994
13. Masilamani S, Kim GH, Mitchell C, Wade JB, Knepper MA: Aldosterone-mediated regulation of ENaC alpha, beta, and gamma subunit proteins in rat kidney. *J Clin Invest* 104: R19–R23, 1999
14. Ecelbarger CA, Kim GH, Terris J, Masilamani S, Mitchell C, Reyes I, Verbalis JG, Knepper MA: Vasopressin-mediated regulation of epithelial sodium channel abundance in rat kidney. *Am J Physiol Renal Physiol* 279: F46–F53, 2000
15. Epstein M, Levinson R, Sancho J, Haber E, Re R: Characterization of the renin-aldosterone system in decompensated cirrhosis. *Circ Res* 41: 818–829, 1977
16. Albiston AL, Obeyesekere VR, Smith RE, Krozowski ZS: Cloning and tissue distribution of the human 11 beta-hydroxysteroid dehydrogenase type 2 enzyme. *Mol Cell Endocrinol* 105: R11–R17, 1994
17. Bostanjoglo M, Reeves WB, Reilly RF, Velazquez H, Robertson N, Litwack G, Morsing P, Dorup J, Bachmann S, Ellison DH, Bostonjoglo M: 11beta-Hydroxysteroid dehydrogenase, mineralocorticoid receptor, and thiazide-sensitive Na-Cl cotransporter expression by distal tubules. *J Am Soc Nephrol* 9: 1347–1358, 1998
18. Funder JW, Pearce PT, Smith R, Smith AI: Mineralocorticoid action: Target tissue specificity is enzyme, not receptor, mediated. *Science* 242: 583–585, 1988
19. Edwards CR, Stewart PM, Burt D, Brett L, McIntyre MA, Sutanto WS, de Kloet ER, Monder C: Localisation of 11 beta-hydroxysteroid dehydrogenase—Tissue specific pro-

tector of the mineralocorticoid receptor. *Lancet* 2: 986–989, 1988
20. Dave-Sharma S, Wilson RC, Harbison MD, Newfield R, Azar MR, Krozowski ZS, Funder JW, Shackleton CH, Bradlow HL, Wei JQ, Hertecant J, Moran A, Neiberger RE, Balfe JW, Fattah A, Daneman D, Akkurt HI, De Santis C, New MI: Examination of genotype and phenotype relationships in 14 patients with apparent mineralocorticoid excess. *J Clin Endocrinol Metab* 83: 2244–2254, 1998
21. Kotelevtsev Y, Brown RW, Fleming S, Kenyon C, Edwards CR, Seckl JR, Mullins JJ: Hypertension in mice lacking 11beta-hydroxysteroid dehydrogenase type 2. *J Clin Invest* 103: 683–689, 1999
22. Biller KJ, Unwin RJ, Shirley DG: Distal tubular electrolyte transport during inhibition of renal 11beta-hydroxysteroid dehydrogenase. *Am J Physiol Renal Physiol* 280: F172–F179, 2001
23. Jonassen TE, Christensen S, Kwon TH, Langhoff S, Salling N, Nielsen S: Renal water handling in rats with decompensated liver cirrhosis. *Am J Physiol Renal Physiol* 279: F1101–F1109, 2000
24. Kim SW, Wang W, Nielsen J, Praetorius J, Kwon TH, Knepper MA, Frokiaer J, Nielsen S: Increased expression and apical targeting of renal ENaC subunits in puromycin aminonucleoside-induced nephrotic syndrome in rats. *Am J Physiol Renal Physiol* 286: F922–F935, 2004
25. Christensen BM, Zelenina M, Aperia A, Nielsen S: Localization and regulation of PKA-phosphorylated AQP2 in response to V(2)-receptor agonist/antagonist treatment. *Am J Physiol Renal Physiol* 278: F29–F42, 2000
26. Perez TR: Is cirrhosis of the liver experimentally produced by CCl4 and adequate model of human cirrhosis? *Hepatology* 3: 112–120, 1983
27. Vallet V, Chraibi A, Gaeggeler HP, Horisberger JD, Rossier BC: An epithelial serine protease activates the amiloride-sensitive sodium channel. *Nature* 389: 607–610, 1997
28. Kim GH, Masilamani S, Turner R, Mitchell C, Wade JB, Knepper MA: The thiazide-sensitive Na-Cl cotransporter is an aldosterone-induced protein. *Proc Natl Acad Sci U S A* 95: 14552–14557, 1998
29. Nielsen J, Kwon TH, Praetorius J, Kim YH, Frokiaer J, Knepper MA, Nielsen S: Segment-specific ENaC downregulation in kidney of rats with lithium-induced NDI. *Am J Physiol Renal Physiol* 285: F1198–F1209, 2003
30. Farman N, Rafestin-Oblin ME: Multiple aspects of mineralocorticoid selectivity. *Am J Physiol Renal Physiol* 280: F181–F192, 2001
31. Bernardi M, Trevisani F, Gasbarrini A, Gasbarrini G: Hepatorenal disorders: Role of the renin-angiotensin-aldosterone system. *Semin Liver Dis* 14: 23–34, 1994
32. Kagawa CM, Cella JA, Van Arman CG: Action of new steroids in blocking effects of aldosterone and desoxycorticosterone on salt. *Science* 126: 1015–1016, 1957
33. Bankir L, Martin H, Dechaux M, Ahloulay M: Plasma cAMP: A hepatorenal link influencing proximal reabsorption and renal hemodynamics? *Kidney Int* 59: S50–S56, 1997
34. Wensing G, Sabra R, Branch RA: Renal and systemic hemodynamics in experimental cirrhosis in rats: Relation to hepatic function. *Hepatology* 12: 13–19, 1990
35. Escher G, Nawrocki A, Staub T, Vishwanath BS, Frey BM, Reichen J, Frey FJ: Down-regulation of hepatic and renal 11 beta-hydroxysteroid dehydrogenase in rats with liver cirrhosis. *Gastroenterology* 114: 175–184, 1998
36. Quattropani C, Vogt B, Odermatt A, Dick B, Frey BM, Frey FJ: Reduced activity of 11 beta-hydroxysteroid dehydrogenase in patients with cholestasis. *J Clin Invest* 108: 1299–1305, 2001
37. White PC, Mune T, Agarwal AK: 11beta-ydroxysteroid dehydrogenase and the syndrome of apparent mineralocorticoid excess. *Endocr Rev* 18: 135–156, 1997
38. Jonassen TE, Marcussen N, Haugan K, Skyum H, Christensen S, Andreasen F, Petersen JS: Functional and structural changes in the thick ascending limb of Henle's loop in rats with liver cirrhosis. *Am J Physiol* 273: R568–R577, 1997
39. Jonassen TE, Petersen JS, Sorensen AM, Andreasen F, Christensen S: Aldosterone receptor blockade inhibits increased furosemide-sensitive sodium reabsorption in rats with liver cirrhosis. *J Pharmacol Exp Ther* 287: 931–936, 1998
40. Bailly C, Imbert-Teboul M, Chabardes D, Hus-Citharel A, Montegut M, Clique A, Morel F: The distal nephron of rat kidney: A target site for glucagon. *Proc Natl Acad Sci U S A* 77: 3422–3424, 1980
41. Sasaki S, Imai M: Effects of vasopressin on water and NaCl transport across the in vitro perfused medullary thick ascending limb of Henle's loop of mouse, rat, and rabbit kidneys. *Pflugers Arch* 383: 215–221, 1980
42. Ito O, Kondo Y, Takahashi N, Kudo K, Igarashi Y, Omata K, Imai Y, Abe K: Insulin stimulates NaCl transport in isolated perfused MTAL of Henle's loop of rabbit kidney. *Am J Physiol* 267: F265–F270, 1994
43. Jonassen TE, Sorensen AM, Petersen JS, Andreasen F, Christensen S: Increased natriuretic efficiency of furosemide in rats with carbon tetrachloride-induced cirrhosis. *Hepatology* 31: 1224–1230, 2000
44. Fujita N, Ishikawa SE, Sasaki S, Fujisawa G, Fushimi K, Marumo F, Saito T: Role of water channel AQP-CD in water retention in SIADH and cirrhotic rats. *Am J Physiol* 269: F926–F931, 1995
45. Asahina Y, Izumi N, Enomoto N, Sasaki S, Fushimi K, Marumo F, Sato C: Increased gene expression of water channel in cirrhotic rat kidneys. *Hepatology* 21: 169–173, 1995
46. Fernandez-Llama P, Jimenez W, Bosch-Marce M, Arroyo V, Nielsen S, Knepper MA: Dysregulation of renal aquaporins and Na-Cl cotransporter in CCl4-induced cirrhosis. *Kidney Int* 58: 216–228, 2000
47. Ivarsen P, Frokiaer J, Aagaard NK, Hansen EF, Bendtsen F, Nielsen S, Vilstrup H: Increased urinary excretion of aquaporin 2 in patients with liver cirrhosis. *Gut* 52: 1194–1199, 2003